

# Role of P2 purinergic receptors in synaptic transmission under normoxic and ischaemic conditions in the CA1 region of rat hippocampal slices

Elisabetta Coppi · Anna Maria Pugliese ·  
Holger Stephan · Christa E. Müller · Felicita Pedata

Received: 7 August 2006 / Accepted: 20 November 2006 / Published online: 3 January 2007  
© Springer Science + Business Media B.V. 2007

**Abstract** The role of ATP and its stable analogue ATP $\gamma$ S [adenosine-5'-o-(3-thio)triphosphate] was studied in rat hippocampal neurotransmission under normoxic conditions and during oxygen and glucose deprivation (OGD). Field excitatory postsynaptic potentials (fEPSPs) from the dendritic layer or population spikes (PSs) from the soma were extracellularly recorded in the CA1 area of the rat hippocampus. Exogenous application of ATP or ATP $\gamma$ S reduced fEPSP and PS amplitudes. In both cases the inhibitory effect was blocked by the selective A<sub>1</sub> adenosine receptor antagonist DPCPX (8-cyclopentyl-1,3-dipropylxanthine) and was potentiated by different ecto-ATPase inhibitors: ARL 67156 (6-*N,N*-diethyl-D- $\beta$ , $\gamma$ -dibromomethylene), BGO 136 (1-hydroxynaphthalene-3,6-disulfonate) and PV4 [hexapotassium dihydrogen monotitanoun-decatungstocobaltate(II) tridecahydrate, K<sub>6</sub>H<sub>2</sub>[TiW<sub>11</sub>CoO<sub>40</sub>] $\cdot$ 13H<sub>2</sub>O]. ATP $\gamma$ S-mediated inhibition was reduced by the P2 antagonist suramin [8-(3-benzamido-4-methylbenzamido)naphthalene-1,3,5-trisulfonate] at the somatic level and by other P2

blockers, PPADS (pyridoxalphosphate-6-azophenyl-2',4'-disulfonate) and MRS 2179 (2'-deoxy-*N*<sup>6</sup>-methyladenosine 3',5'-bisphosphate), at the dendritic level. After removal of both P2 agonists, a persistent increase in evoked synaptic responses was recorded both at the dendritic and somatic levels. This effect was prevented in the presence of different P2 antagonists. A 7-min OGD induced tissue anoxic depolarization and was invariably followed by irreversible loss of fEPSP. PPADS, suramin, MRS2179 or BBG (brilliant blue G) significantly prevented the irreversible failure of neurotransmission induced by 7-min OGD. Furthermore, in the presence of these P2 antagonists, the development of anoxic depolarization was blocked or significantly delayed. Our results indicate that P2 receptors modulate CA1 synaptic transmission under normoxic conditions by eliciting both inhibitory and excitatory effects. In the same brain region, P2 receptor stimulation plays a deleterious role during a severe OGD insult.

**Key words** ecto-ATPase inhibitors · extracellular recordings · hippocampal slices · OGD · P2 purinergic receptors · synaptic potentials

E. Coppi · A. M. Pugliese · F. Pedata (✉)  
Department of Preclinical and Clinical Pharmacology,  
University of Florence,  
Viale Pieraccini 6,  
50139 Florence, Italy  
e-mail: felicita.pedata@unifi.it

H. Stephan  
Research Centre Rossendorf, Institute of Radiopharmacy,  
01314 Dresden, Germany

C. E. Müller  
Pharmaceutical Institute, Pharmaceutical Sciences Bonn (PSB),  
University of Bonn,  
An der Immenburg 4,  
53121 Bonn, Germany

## Abbreviations

aCSF	artificial cerebrospinal fluid
AD	anoxic depolarization
ARL 67156	6- <i>N,N</i> -diethyl-D- $\beta$ , $\gamma$ -dibromomethylene ATP
ATP $\gamma$ S	adenosine-5'-o-(3-thio)triphosphate
BBG	brilliant blue G
BGO	136 1-hydroxynaphthalene-3,6-disulfonate
CNS	central nervous system
DC	direct current
DMSO	dimethylsulphoxide
DPCPX	8-cyclopentyl-1,3-dipropylxanthine

fEPSP	field excitatory postsynaptic potential
2meS-ATP	2-methylthio-ATP
MRS 2179	2'-deoxy-N <sup>6</sup> -methyladenosine 3',5'-bisphosphate
OGD	oxygen and glucose deprivation
PPADS	pyridoxalphosphate-6-azophenyl-2',4'-disulfonate
PPF	paired-pulse facilitation
PS	population spike
PV4	hexapotassium dihydrogen monotitanoundecataungstocobaltate(II) tridecahydrate, K <sub>6</sub> H <sub>2</sub> [TiW <sub>11</sub> CoO <sub>40</sub> ]·13H <sub>2</sub> O
RB2	reactive blue 2

## Introduction

The role of adenosine triphosphate (ATP) as a neurotransmitter has been largely demonstrated both in the peripheral and the central nervous system (CNS) (for a review, see: [1]). In the hippocampus, ATP is released from neurones [2–4] and astrocytes [5, 6] through various mechanisms, including a vesicular mode [7]. ATP triggers pathophysiological responses by stimulating purinergic P2 receptors, classified as P2X and P2Y [1, 8–10]. P2X receptors are ligand-gated ion channels permeable to cations (Na<sup>+</sup>, K<sup>+</sup> and Ca<sup>2+</sup>) that are present as homo- and heteromeric trimers on the cell surface [11, 12]. Seven different subunits of P2X purinergic receptors (P2X<sub>1–7</sub>) have been cloned to date in mammals. P2Y receptors are G protein-coupled receptors showing the typical structure of a single subunit with seven membrane-spanning domains [13]. Eight subtypes of metabotropic P2Y receptors (P2Y<sub>1,2,4,6,11,12,13,14</sub>, plus the recently orphanized GPR17 receptor by Abbracchio and colleagues: see [14]) have been cloned to date [15]. Both P2X and P2Y receptors are widely expressed in many brain areas, including the hippocampus [16, 17].

Both potentiating and suppressing effects of exogenously applied ATP on synaptic transmission have been reported [18–20], depending on varying expression and localization of purinergic receptor subtypes.

It has been demonstrated that ATP acts as a fast neurotransmitter in the CNS. In fact, P2X-mediated synaptic currents are present in different brain areas: the CA3 [3] and CA1 [21] hippocampal regions, the somatosensory cortex [22], the medial habenula [23], locus coeruleus [24] and neurones of the trigeminal mesencephalic nucleus [25].

At the presynaptic level, P2X receptor activation enhances glutamate [4, 19, 26] and  $\gamma$ -aminobutyric acid (GABA) [27–29] release from neurones in the hippocampus. An excitatory effect of 2-methylthio-ATP (2meS-ATP) and of ATP itself, but only in the presence of 8-cyclopentyl-

1,3-dipropylxanthine (DPCPX), is exerted in neurones of the rat prefrontal cortex [30].

Studies in primary cultures of rat hippocampal cells demonstrated that tonic- and activity-dependent release of ATP by astrocytes can stimulate presynaptic P2Y receptors with a consequent inhibition of glutamate release [5, 6, 31]. Similarly, it has been demonstrated that synaptic transmission is markedly inhibited by exogenous application of ATP and stable analogues in a concentration-dependent way both in hippocampal [32–35] and prefrontal cortex slices [36]. These effects are theophylline sensitive but quite unaffected by suramin, pyridoxalphosphate-6-azophenyl-2',4'-disulfonate (PPADS) and ecto-ATPase/ecto-nucleotidase inhibitors.

It is generally known that extracellular ATP is rapidly converted into adenosine through ecto-nucleotidases [37], with subsequent activation of P1 adenosine receptors. The adenosine A<sub>1</sub> subtype [33, 38] is particularly expressed in the hippocampus. Under physiological conditions, the tonic role of extracellular adenosine in inhibiting CA1 hippocampal neurotransmission through A<sub>1</sub> receptor activation has been well described [39, 40]. First, the inhibition exerted by ATP on hippocampal neurotransmission was attributed to its rapid conversion (<1 s) to adenosine by ecto-ATPases and ecto-nucleotidases and subsequent activation of A<sub>1</sub> receptors based on the observation that this response was theophylline sensitive [32, 33, 41] and absent in A<sub>1</sub> knockout mice [34]. On the other hand, a more detailed observation of adenine nucleotide-evoked effects and the synthesis of new pharmacological tools revealed a P2-mediated inhibition of synaptic transmission in the hippocampus [17, 35, 36].

In general, it appears that P2Y receptor stimulation is mostly associated with an inhibition of synaptic transmission [17, 35, 36], while P2X activation is mainly correlated with an increase in excitatory neurotransmission [3, 4, 21–24, 42, 43].

The relative contribution of P1 and P2 receptor activation to the total hippocampal neurotransmission is still to be clarified (see [17, 34]).

The role of P2 receptors may become relevant during pathological conditions such as ischaemia. Evidence of an increased outflow of radioactive ATP from hippocampal slices during ischaemic-like conditions was reported by Juranyi et al. [44] and the first demonstration that ATP outflow increases *in vivo* during the induction of focal ischaemia in the rat was reported by Melani et al. [45]. Evidence supports the idea that, under such pathological conditions, released ATP may exert a cytotoxic role. Intraatrial ATP injection in rats induced, 24 h later, a clearly lesioned area [46]. The ATP-induced damage was concentration-dependent, mimicked by ATP $\gamma$ S and  $\alpha,\beta$ meATP (but not by ADP or adenosine) and blocked by

reactive blue 2 (RB2), a non-specific P2 antagonist [47]. Suramin, another non-specific P2 receptor antagonist, administered 30 min before occlusion of the middle cerebral artery, resulted in a significant decrease in infarct and oedema volume 6 h after brain injury [47]. In agreement, it has been demonstrated that RB2 [48] and PPADS [49] improve the neurological deficit and reduce the damage induced in rats in a model of focal ischaemia *in vivo*. Protective effects of P2 receptor antagonists [suramin, brilliant blue G (BBG) and RB2] on cell survival were also demonstrated in organotypic hippocampal slices exposed to oxygen and glucose deprivation (OGD) [50, 51].

In this work we investigated the role of P2 purinergic receptor activation in CA1 neurotransmission in rat hippocampal slices under normoxic and ischaemia-like conditions, through the application of different P2 purinergic receptor agonists and antagonists.

## Methods

All animal procedures were conducted according to the European Community Guidelines for Animal Care, DL 116/92, application of the European Communities Council Directive (86/609/EEC). Experiments were carried out on acute rat hippocampal slices, prepared as previously described [52, 53].

### Preparation of slices

Male Wistar rats (Harlan Italy, Udine, Italy, 150–200 g body weight) were anaesthetized with ether and decapitated with a guillotine. The hippocampi were rapidly removed and placed in ice-cold oxygenated (95% O<sub>2</sub>–5% CO<sub>2</sub>) artificial cerebrospinal fluid (aCSF) of the following composition (mM): NaCl 124, KCl 3.33, KH<sub>2</sub>PO<sub>4</sub> 1.25, MgSO<sub>4</sub> 1.4, CaCl<sub>2</sub> 2.5, NaHCO<sub>3</sub> 25 and D-glucose 10. Slices (400 μm nominal thickness) were cut using a McIlwain tissue chopper (Mickle Laboratory Engineering, Co. Ltd., Gomshall, UK) and kept in oxygenated aCSF for at least 1 h at room temperature. A single slice was then placed on a nylon mesh, completely submerged in a small chamber (0.8 ml) and superfused with oxygenated aCSF (30–32°C) at a constant flow rate of 1.5 ml min<sup>-1</sup>. The treated solutions reached the preparation in 60 s and this delay was taken into account in our calculations.

### Extracellular recordings

Test pulses (80 μs, 0.066 Hz) were delivered through a bipolar nichrome electrode positioned in the stratum radiatum of the CA1 region of the hippocampus to stimulate the Schaffer collateral-commissural pathway.

Evoked potentials were extracellularly recorded with glass microelectrodes (2–10 MΩ, Clark Electromedical Instruments, Pangbourne, UK) filled with 150 mM NaCl. The recording electrode was placed at the soma or at the dendritic level of the CA1 region to record population spikes (PSs) or field excitatory postsynaptic potentials (fEPSPs), respectively. Responses were amplified (BM 622, Mangoni, Pisa, Italy), digitized (sample rate: 33.33 kHz), low-pass filtered in direct current (DC) mode at 10 kHz and stored for later analysis using LTP software facilities (version 2.30D, William W. Anderson, 1991–2001).

The amplitude of fEPSP was measured as the difference between the negative peak following the afferent fibre volley and the baseline value preceding the stimulus artefact. In some experiments both the amplitude and the initial slope of fEPSP were quantified, but since no appreciable difference between these two parameters was observed under control conditions, in the presence of drugs or during *in vitro* ischaemia, only the measure of the amplitude was expressed in figures. The amplitude of PS was measured as the difference between the peak negativity and the averaged values of the two peak positivities following the stimulus artefact.

When a stable baseline of evoked responses was reached, fEPSP or PS amplitudes were routinely measured and expressed as the percentage of the mean value recorded 5 min before the application of any treatment.

Stimulus-response curves were obtained by gradual increase in stimulus strength at the beginning and at representative times during each experiment, as indicated in the “Results” section. The test stimulus strength was then adjusted to produce a response whose amplitude was 40–50% of the maximum and was kept constant throughout the experiment.

In a group of slices, simultaneously with fEPSP amplitude, we also recorded anoxic depolarization (AD) as negative shifts in the DC mode induced by 7-min OGD.

### OGD conditions

Slices were perfused for 7 min with aCSF without glucose and gassed with nitrogen (95% N<sub>2</sub>–5% CO<sub>2</sub>: OGD) as indicated elsewhere [52, 53]. The effects of 7-min OGD in hippocampal slices were evaluated by recording fEPSP amplitude according to a previously described method [52, 53]. In a typical experimental day, a control slice was submitted to 7 min of OGD. If the recovery of fEPSP amplitude after 15 min of reperfusion with glucose-containing and normally oxygenated aCSF was ≤15% of the preischaemic value, a second slice from the same rat was submitted to a 7-min OGD insult in the presence of the P2 antagonist under investigation. To confirm the result obtained in the treated group, a third slice was taken from the same rat and another 7-min OGD was performed under

control conditions to verify that no difference between slices was caused by the time gap between the experiments.

#### Drug application

Under normoxic conditions, ATP and its metabolically stable analogue ATP $\gamma$ S were applied by superfusion for 10 min, a time that allowed us to record a stable response to the compounds. The P2 purinergic antagonists (suramin, PPADS, MRS 2179 and BBG) were applied 10 or 15 min before, during and 5 min after the application of P2 agonists or the induction of OGD.

Ecto-ATPases (NTPDase1, 2 and 3) are responsible for the degradation of extracellular ATP [54]. In the present work, three different ecto-ATPase inhibitors were tested: ARL 67156, BGO 136 and PV4. ARL 67156, a commonly used ecto-ATPase inhibitor [55], was superfused at a concentration of 50  $\mu$ M, 20 min before and during ATP or ATP $\gamma$ S application, in accordance with previous data in the literature [43, 56]. However, it has been recently shown that, at micromolar concentrations, ARL 67156 only inhibits rat NTPDase1 and 3 transiently transfected in Chinese hamster ovary cells, showing negligible activity on NTPDase2 [57]. In addition, a possible interaction of this ATP analogue with some P2Y receptors has been suggested [58]. BGO 136 is a new ecto-ATPase inhibitor recently available commercially. From the few data existing in the literature at present, this compound is described as a selective NTPDase1 and 2 blocker with  $K_i$  values in the high micromolar range [59], being ineffective at concentrations below 5 mM ([60] and our unpublished observation). PV4 is a recently synthesized compound (not available commercially) that belongs to a new class of ecto-ATPase inhibitors: the polyoxotungstates [61]. PV4 strongly inhibits rat NTPDase1, 2 and 3 with  $K_i$  values in the nanomolar range [61]. Its high affinity for these enzymes renders it a useful tool (the best one available at present) to inhibit extracellular ATP catabolism without interfering with P2Y receptors, at least at 10  $\mu$ M concentrations [61]. Since no data are available at present about the application of BGO 136 or PV4 to brain slices, for similarity with ARL 67156 we superfused these compounds 20 min before ATP application. In some cases hippocampal slices were preincubated in the presence of the ecto-ATPase inhibitors 1 h before starting the experiment, but since no significant difference was found with non-incubated slices, the results were pooled together.

Suramin is a non-specific and non-competitive antagonist of P2 purinergic receptors (either P2X or P2Y). It also inhibits ecto-nucleotidase activity [57] and affects glutamatergic and GABAergic receptor activation in rat hippocampal slices [62]. PPADS is an antagonist at both P2Y (P2Y<sub>1,2,4,6</sub>) and P2X<sub>1-5</sub> receptors and is the compound most

used to block P2 purinergic receptor activation [1, 49]. BBG is a selective P2X<sub>7</sub> receptor antagonist [63, 64]. MRS 2179 is a selective P2Y<sub>1</sub> purinergic antagonist, at least at concentrations below 1  $\mu$ M [65, 66].

The concentrations used for each antagonist were chosen on the basis of  $K_i$  values evaluated at rat P2 receptors [1, 67, 68].

All the P2 purinergic agonists and antagonists were dissolved in distilled water and stock solutions at 100–10,000 times the desired final concentration were stored at  $-20^{\circ}\text{C}$ . The drugs were dissolved in aCSF at the required concentration immediately before superfusion.

DPCPX was dissolved in dimethylsulphoxide (DMSO) and stock solutions were made to obtain concentrations of DMSO lower than 0.001% in the superfusing aCSF. Control experiments, carried out in parallel, showed that this concentration of DMSO did not affect CA1 hippocampal neurotransmission.

#### Paired-pulse facilitation

To elicit paired-pulse facilitation (PPF) of fEPSP, we stimulated the Schaffer collateral-commissural fibres twice with a 40-ms interpulse interval. The synaptic facilitation was quantified as the ratio (P2/P1) between the amplitude of the fEPSP elicited by the second (P2) and the first (P1) stimuli. When applied, PPF was monitored for at least 5 min before, during and after the application of each drug. The effects of ATP and ATP $\gamma$ S on PPF were evaluated by measuring the P2/P1 ratio obtained before, during and 10 min after agonist application.

#### Chemicals

ATP (adenosine 5'-triphosphate), ATP $\gamma$ S [adenosine 5'-O-(3-thiotriphosphate)], BBG (brilliant blue G) and BGO 136 (1-hydroxynaphthalene-3,6-disulfonic acid) were purchased from Sigma (Milan, Italy). PPADS (pyridoxalphosphate-6-azophenyl-2',4'-disulfonic acid tetrasodium salt), ARL 67156 (6-*N,N*-diethyl-D- $\beta$ , $\gamma$ -dibromomethylene ATP), suramin [8-(3-benzamido-4-methylbenzamido)naphthalene-1,3,5-trisulfonic acid] and MRS 2179 (2'-deoxy-*N*<sup>6</sup>-methyladenosine 3',5'-bisphosphate tetraammonium salt) were obtained from Tocris (Bristol, UK). DPCPX (8-cyclopentyl-1,3-dipropylxanthine) was purchased from Research Biochemicals International (Natick, MA, USA). PV4 (hexapotassium dihydrogen monotitanoundecatungstocobaltate (II) tridecahydrate,  $\text{K}_6\text{H}_2[\text{TiW}_{11}\text{CoO}_{40}]\cdot 13\text{H}_2\text{O}$ ) was synthesized as described [69, 70].

#### Statistical analysis

Data were analyzed using Prism 3.02 software (Graphpad Software, San Diego, CA, USA). All numerical data are

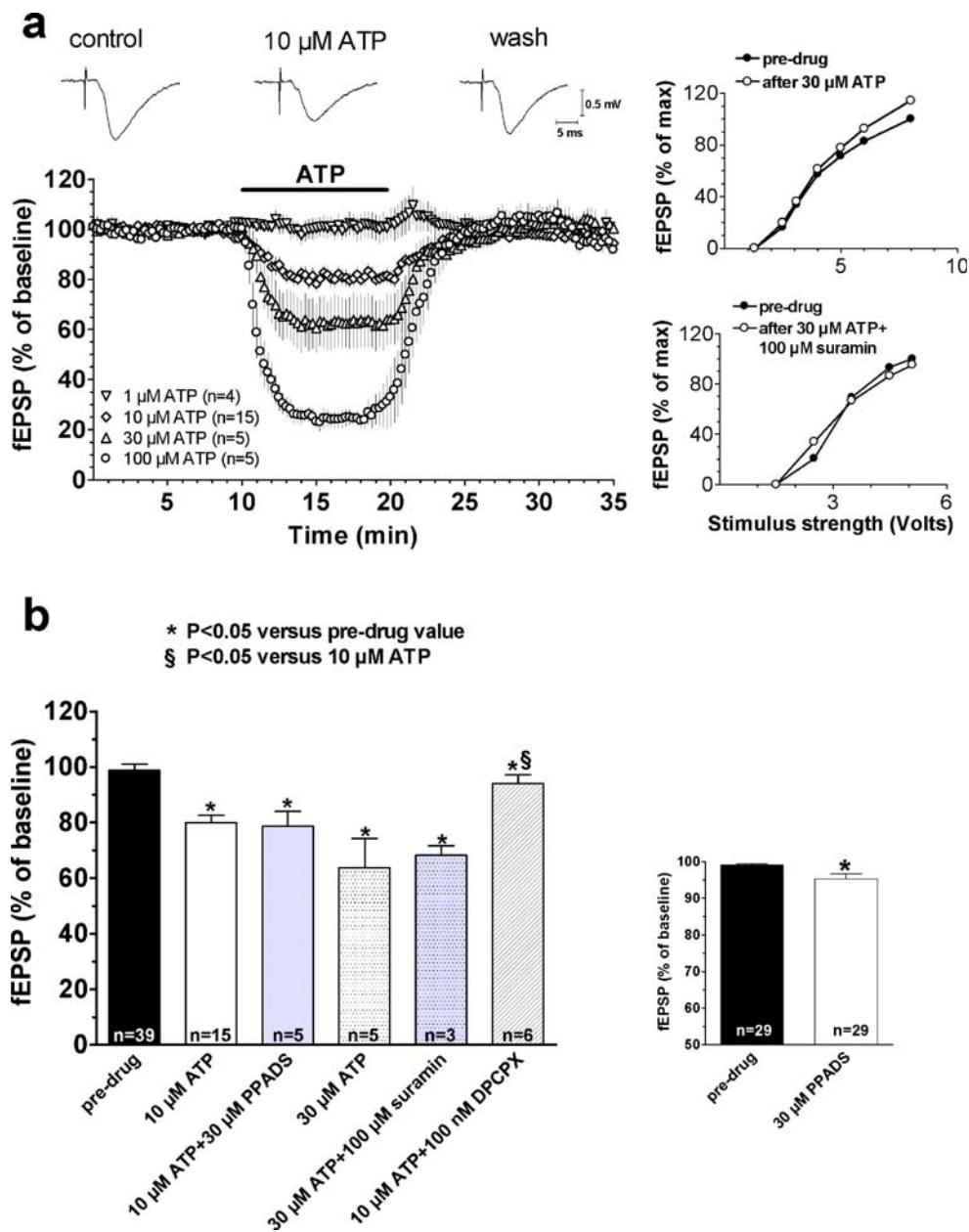


**Fig. 1** The inhibitory effect induced by ATP on fEPSP amplitude is not blocked by P2 purinergic antagonists. **a** Time course of fEPSP amplitude before, during and after the application of different concentrations of ATP. Each point in the graph represents the mean  $\pm$  SE of fEPSP value measured as percent of baseline, pre-drug level. Note that ATP was ineffective at 1  $\mu$ M, whereas a significant inhibition of fEPSP amplitude was observed starting from a concentration of 10  $\mu$ M ( $P < 0.05$ , paired Student's *t*-test). *Upper panels* represent single traces recorded in a typical experiment before, during and after 10  $\mu$ M ATP application. *Upper inset*: stimulus-response curves recorded before and after 30  $\mu$ M ATP application illustrate the potentiating effect of the P2 agonist on a wide range of stimulus strengths in a typical experiment. fEPSP amplitude is expressed as percent of the maximal value obtained under control conditions at the highest stimulus strength. Note the increase in fEPSP amplitude recorded 15 min after 30  $\mu$ M ATP removal at stimulus intensities able

to evoke more than 50% of the maximal response. *Lower inset*: the potentiating effect was prevented in the presence of 100  $\mu$ M suramin. **b** *Columns* in the graph summarize the average amplitude (mean  $\pm$  SE) of evoked fEPSP recorded from hippocampal slices under control conditions, 5 min after superfusion of ATP alone and 5 min after ATP superfusion in the presence of different purinergic antagonists. Note that the inhibitory effect of ATP on fEPSP amplitude is not blocked by the P2 antagonists PPADS and suramin, but only by the A<sub>1</sub> adenosine antagonist, DPCPX. \* $P < 0.05$ , one-way ANOVA followed by Newman-Keuls test versus pre-drug value. § $P < 0.05$ , one-way ANOVA followed by Newman-Keuls test versus 10  $\mu$ M ATP-treated slices. *Inset*: *bars* in the graph represent the average of fEPSP amplitude 5 min before and during the last 5 min of PPADS superfusion (30  $\mu$ M). A significant difference was found between the two values (\* $P < 0.05$ , paired Student's *t*-test)

expressed as the mean  $\pm$  SE. Data were tested for statistical significance with the paired two-tailed Student's *t*-test or by analysis of variance (one-way ANOVA), as appropriate. When significant differences were observed, the Newman-Keuls multiple comparison test (one-way ANOVA) was done. A value of  $P < 0.05$  was considered significant.

## Results

### Effects of ATP on CA1 hippocampal neurotransmission

In a first series of experiments, the effect of ATP on evoked synaptic transmission in the CA1 region of rat hippocampal slices was investigated. Figure 1a shows that a 10-min application of ATP decreased the evoked fEPSP amplitude in a concentration-dependent manner. A partial but statistically significant inhibition was observed at a concentration of 10  $\mu$ M ATP ( $20.3 \pm 2.5$ ,  $P < 0.0001$ , paired Student's *t*-test), while an almost complete inhibition was observed at a concentration of 100  $\mu$ M ATP ( $77.8 \pm 3.3\%$ ). As shown in Fig. 1a, the effect was always reversible after a few minutes of washout. The apparent  $EC_{50}$  value of ATP on fEPSP inhibition was 59  $\mu$ M [95% confidence limits (CL): 17–198  $\mu$ M]. These data are in line with previous results demonstrating an ATP-mediated inhibition of extracellularly recorded CA1 neurotransmission [32–35, 41]. At the beginning of each experiment and 15 min after ATP washout, a stimulus-response curve was delivered to verify if there was a relatively “long-lasting” potentiation of synaptic responses after ATP removal. Such an effect has already been reported to occur in hippocampal slices [41, 71–76]. At concentrations of 1–10  $\mu$ M we did not observe any change in fEPSP amplitude after a 15-min application of ATP at any stimulus intensity tested (data not shown). On the contrary, an increase of  $6.6 \pm 3.8\%$  and of  $12.3 \pm 7.2\%$  in fEPSP amplitude was observed at the highest stimulus intensity tested after 30  $\mu$ M (upper inset of Fig. 1a) and 100  $\mu$ M ATP superfusion, respectively.

The inhibitory effect of ATP on fEPSP amplitude was not blocked by the P2 antagonists PPADS and suramin (Fig. 1b). The two compounds were applied 10 min before, during and 5 min after ATP superfusion. As shown in Fig. 1b, 10  $\mu$ M ATP in the presence of 30  $\mu$ M PPADS still elicited a fEPSP inhibition of  $20 \pm 9\%$ , which is not different from that obtained with ATP alone. Similarly, 30  $\mu$ M ATP in the presence of 100  $\mu$ M suramin evoked a  $32 \pm 3.5\%$  fEPSP inhibition, which is not different from the  $36 \pm 10.6\%$  fEPSP reduction obtained with 30  $\mu$ M ATP alone. The potentiation induced by 30  $\mu$ M ATP was blocked in the presence of 100  $\mu$ M suramin (lower inset of Fig. 1a). It should be noted that PPADS alone, but not suramin, significantly reduced fEPSP amplitude of  $5.21 \pm 1.6\%$  (inset

of Fig. 1b;  $P < 0.05$ , paired Student's *t*-test,  $n = 29$ ) in accordance with previous data obtained in the rat hippocampus [43, 21] and prefrontal cortex [30, 36].

It is well known that extracellular ATP is rapidly metabolized by membrane ecto-ATPases, leading to the formation of ADP, AMP and adenosine. Adenosine  $A_1$  receptors are highly distributed in the CA1 hippocampus and many effects of exogenous ATP have been attributed to  $A_1$  adenosine receptor activation after ATP catabolism in this brain region. For this reason, the effect of ATP was also evaluated in the presence of the selective adenosine  $A_1$  antagonist DPCPX. The application of 100 nM DPCPX 30 min before ATP superfusion significantly increased fEPSP amplitude ( $12.7 \pm 5.2\%$  vs control,  $n = 5$ ,  $P < 0.05$ , paired Student's *t*-test, data not shown). In addition, it completely blocked the ATP-mediated reduction of fEPSP ( $P < 0.05$ , one-way ANOVA, Newman-Keuls post test, Fig. 1b). We also investigated the effect of ATP in the presence of different ecto-ATPase inhibitors: ARL 67156, BGO 136 and PV4. As illustrated in Fig. 2, in the presence of all these compounds the inhibitory effect on fEPSP amplitude elicited by 10  $\mu$ M ATP ( $35.8 \pm 6.4\%$  in ATP + ARL 67156,  $n = 5$ ;  $38.2 \pm 3.6\%$  in ATP + BGO 136,  $n = 5$ ;  $35.2 \pm 6.1\%$  in ATP + PV4,  $n = 6$ ) was significantly enhanced

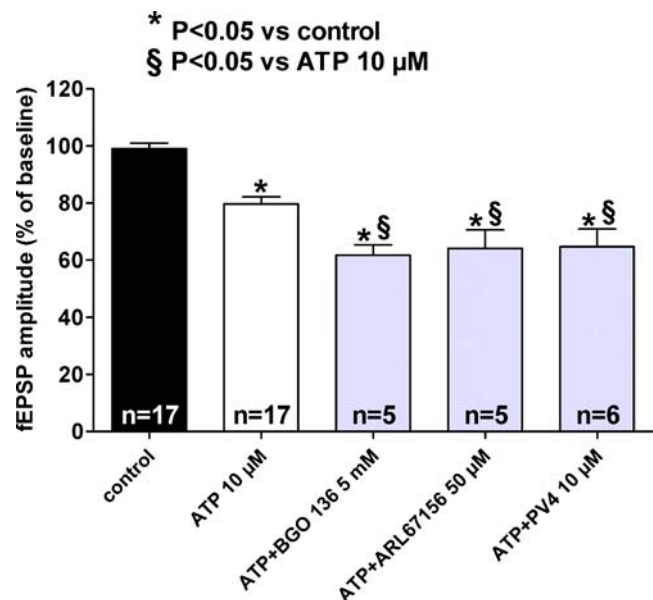


**Fig. 2** The inhibitory effect induced by ATP on fEPSP amplitude is potentiated in the presence of different ecto-ATPases inhibitors. Columns in the graph summarize the average amplitude (mean  $\pm$  SE) of evoked fEPSP recorded from hippocampal slices under control conditions, 5 min after superfusion of ATP alone and 5 min after ATP superfusion in the presence of different ecto-ATPases inhibitors. Note that the inhibitory effect of ATP on fEPSP amplitude is potentiated by BGO 136, PV4 and ARL 67156. \* $P < 0.05$  one-way ANOVA, followed by Newman-Keuls test versus pre-drug value. § $P < 0.05$ , one-way ANOVA followed by Newman-Keuls test versus 10  $\mu$ M ATP-treated slices

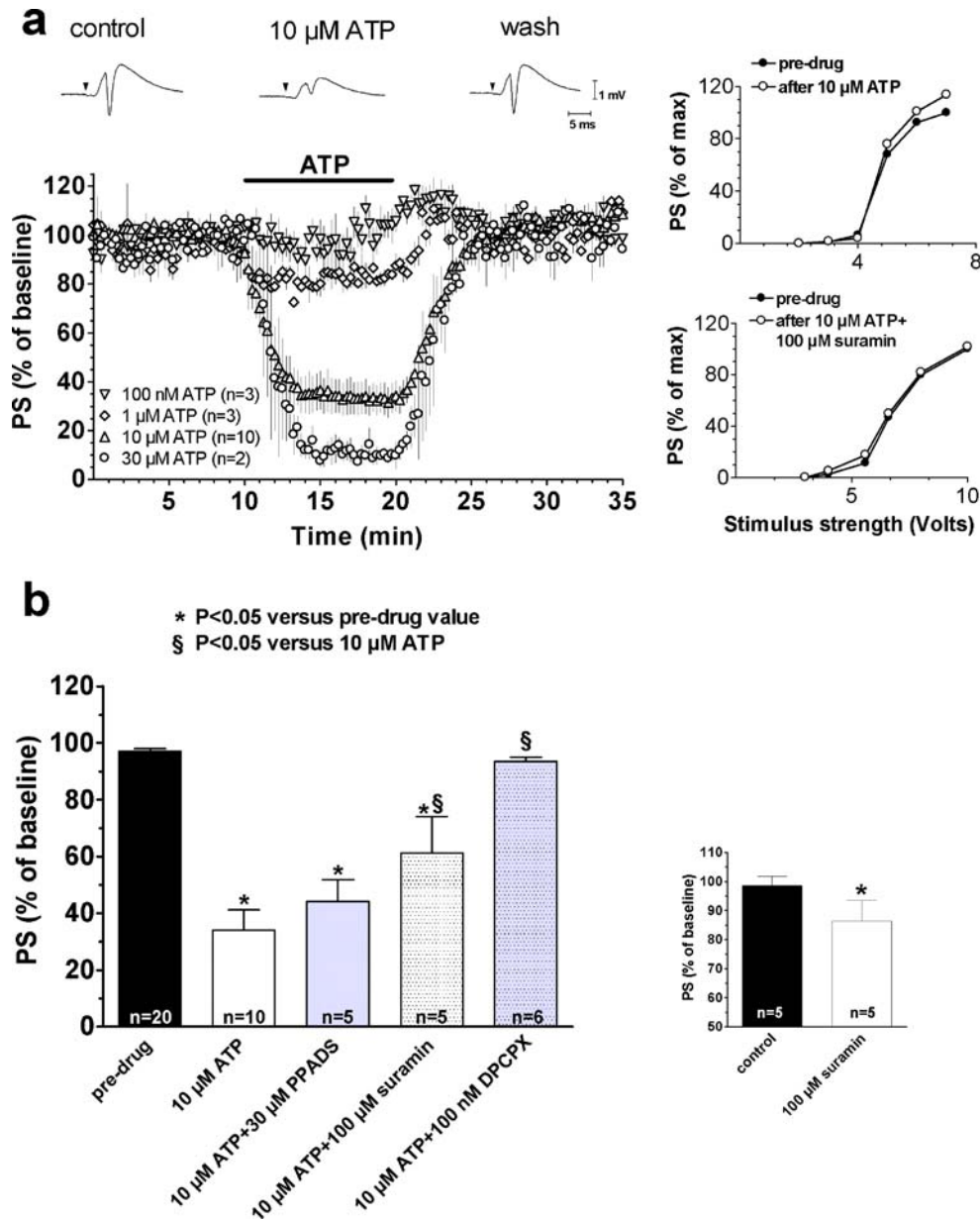


**Fig. 3** The inhibitory effect induced by ATP on PS amplitude is blocked by DPCPX, a selective  $A_1$  adenosine receptor antagonist, and by suramin, an aspecific P2 antagonist. **a** Time course of PS amplitude before, during and after the application of different concentrations of ATP. Each point in the graph represents the mean  $\pm$  SE of the PS value measured as percent of baseline, pre-drug level. Note that the P2 agonist was ineffective at 100 nM, whereas a significant inhibition of fEPSP amplitude was observed starting from a concentration of 1  $\mu$ M ( $P < 0.05$ , paired Student's *t*-test). *Upper panels* represent single traces recorded in a typical experiment before, during and after 10  $\mu$ M ATP application. The stimulus artefact was blanked and replaced by the arrowhead. *Upper inset*: stimulus-response curves recorded before and after 10  $\mu$ M ATP application illustrate the potentiating effect of the P2 agonist on a wide range of stimulus strengths in a typical experiment. PS amplitude is expressed as percent of the maximal value obtained under control conditions at the highest stimulus strength. Note the increase in PS amplitude recorded 15 min after 10  $\mu$ M ATP removal at

stimulus intensities able to evoke more than 50% of the maximal response. *Lower inset*: the potentiating effect was prevented in the presence of 100  $\mu$ M suramin. **b** Columns in the graph summarize the average amplitude (mean  $\pm$  SE) of evoked PS recorded from hippocampal slices under control conditions, 5 min after superfusion of ATP alone and 5 min after ATP superfusion in the presence of different drugs. Note that the inhibitory effect of ATP on PS amplitude is not modified by the P2 antagonist PPADS, while it is reduced by the P2 antagonist suramin and is blocked by the  $A_1$  adenosine antagonist DPCPX. \* $P < 0.05$ , one-way ANOVA followed by Newman-Keuls test versus pre-drug value. § $P < 0.05$ , one-way ANOVA followed by Newman-Keuls test versus 10  $\mu$ M ATP-treated slices. *Inset*: bars in the graph represent the average of PS amplitude 5 min before and during the last 5 min of 100  $\mu$ M suramin application. A significant difference was found between the two values (\* $P < 0.05$ , paired Student's *t*-test)

in comparison to that observed with ATP alone ( $20.3 \pm 2.5\%$ ,  $P < 0.05$ , one-way ANOVA, Newman-Keuls post test).

The effects of ATP were also studied by recording synaptic potentials at the somatic level of the CA1 region. ATP (10  $\mu\text{M}$ ) induced a  $66 \pm 7.1\%$  decrease in PS amplitude ( $P < 0.0001$ , paired Student's *t*-test, Fig. 3a) that was reversed after few minutes' washout. The apparent  $\text{EC}_{50}$  value of ATP on PS inhibition was 7  $\mu\text{M}$  (95% CL: 1.5–33  $\mu\text{M}$ ). When the stimulus-response curve was delivered 15 min after drug removal, a significant increase in PS amplitude ( $P < 0.05$ , paired Student's *t*-test,  $n = 7$ ) was observed at a stimulus intensity able to evoke a response higher than 50% of the maximum (upper inset of Fig. 3a). At the highest stimulus intensity tested, the increase was  $14.8 \pm 3\%$  ( $n = 7$ ).

No block of ATP-mediated inhibition of PS amplitude was observed in the presence of PPADS (Fig. 3b). On the contrary, 100  $\mu\text{M}$  suramin significantly blocked the ATP-mediated inhibition of the evoked potentials ( $P < 0.05$ , one-way ANOVA, Newman-Keuls post test, Fig. 3b) and completely prevented the potentiation of the stimulus-response curve (lower inset of Fig. 3a). In addition, it induced a significant decrease in PS amplitude ( $12.8 \pm 3.4\%$ ,  $P < 0.05$ , paired Student's *t*-test) when applied alone (inset of Fig. 3b).

DPCPX (100 nM) applied 30 min before, during and 5 min after ATP superfusion antagonized the effects of 10  $\mu\text{M}$  ATP on PS amplitude, as observed at the dendritic level. DPCPX alone significantly increased PS amplitude ( $60.3 \pm 11.4\%$  vs control PS,  $n = 6$ ,  $P < 0.05$ , paired Student's *t*-test, data not shown).

#### Effects of ATP $\gamma\text{S}$ on CA1 hippocampal neurotransmission

ATP $\gamma\text{S}$ , the metabolically stable ATP analogue, evoked a concentration-dependent decrease in fEPSP amplitude (Fig. 4a). A statistically significant reduction was evident starting from a concentration of 3  $\mu\text{M}$  ( $P < 0.05$ , paired Student's *t*-test), and at 10  $\mu\text{M}$ , ATP $\gamma\text{S}$  inhibited fEPSP amplitude by  $32.6 \pm 4.2\%$  (Fig. 4a). The apparent  $\text{EC}_{50}$  value estimated for ATP $\gamma\text{S}$  on fEPSP inhibition was 22  $\mu\text{M}$  (95% CL: 4.6–106  $\mu\text{M}$ ). In all the slices in which we recorded a stimulus-response curve before and 15 min after ATP $\gamma\text{S}$  application, a statistically significant potentiation of fEPSP ( $P < 0.05$ , paired Student's *t*-test,  $n = 12$ ) was observed at intensities able to evoke a response higher than 50% of the maximum (upper inset of Fig. 4a).

The inhibitory effect of ATP $\gamma\text{S}$  on fEPSP amplitude was significantly reduced both in the presence of 30  $\mu\text{M}$  PPADS and 10  $\mu\text{M}$  MRS 2179. When higher concentrations of PPADS (50  $\mu\text{M}$ , Fig. 4b) and MRS 2179 (30  $\mu\text{M}$ , data not shown) were tested, no significant difference in the block of

ATP $\gamma\text{S}$ -induced inhibition was found. Both antagonists completely prevented the potentiation of the stimulus-response curve observed after 15 min of ATP $\gamma\text{S}$  washout (lower inset of Fig. 4a) at the dendritic level. It should be noted that the application of 10  $\mu\text{M}$  MRS 2179 alone caused a modest but significant reduction in fEPSP amplitude ( $6.1 \pm 3.2\%$ ,  $P < 0.05$ , paired Student's *t*-test, inset of Fig. 4b,  $n = 15$ ). Contrary to PPADS and MRS 2179, the aspecific purinergic antagonist suramin (100  $\mu\text{M}$ ) did not significantly inhibit ATP $\gamma\text{S}$  effects at the dendritic level (Fig. 4b).

Surprisingly, the effect of ATP $\gamma\text{S}$  on fEPSP amplitude was completely antagonized by the selective adenosine  $\text{A}_1$  antagonist, DPCPX (Fig. 4b). Evidence exists that even this metabolically stable ATP analogue is partially converted to adenosine [34]. To verify this possibility, we applied ATP $\gamma\text{S}$  after a 30-min application of 50  $\mu\text{M}$  ARL 67156. However, under these experimental conditions, a 10-min application of ATP $\gamma\text{S}$  induced an even more pronounced effect on evoked neurotransmission (Fig. 4b). In fact, the reduction in fEPSP amplitude elicited by 10  $\mu\text{M}$  ATP $\gamma\text{S}$  in the presence of ARL 67156 was  $68.2 \pm 4.6\%$ , which is significantly greater than that observed under control conditions ( $P < 0.001$ , one-way ANOVA, Newman-Keuls post test).

At the somatic level, we delivered a cumulative concentration-response curve (Fig. 5a) for ATP $\gamma\text{S}$ , since no desensitization was observed during single drug applications (data not shown). Also in this case, the exogenous application of ATP $\gamma\text{S}$  produced a concentration-dependent decrease in PS amplitude. A significant effect was observed starting from a concentration of 3  $\mu\text{M}$  ( $17.4 \pm 8.6\%$ ,  $P < 0.05$ , paired Student's *t*-test), while at a 30  $\mu\text{M}$  concentration PS was completely suppressed. The apparent  $\text{EC}_{50}$  value for ATP $\gamma\text{S}$  on PS inhibition was 6  $\mu\text{M}$  (95% CL: 1.2–28  $\mu\text{M}$ ). Under these experimental conditions, a potentiation of PS amplitude ( $37 \pm 12.1\%$ ) was observed after drug removal in comparison to pre-drug values (see Fig. 5a, trace f) even without eliciting a stimulus-response curve. The potentiation of somatic response persisted for at least 30 min and was also recorded during the stimulus-response curve (inset of Fig. 5a) after 15 min of washout.

The application of 30  $\mu\text{M}$  PPADS was unable to block the ATP $\gamma\text{S}$ -mediated inhibition of PS amplitude (Fig. 5b) and did not affect the potentiation of the stimulus-response curve observed 15 min after drug removal (data not shown). On the contrary, suramin (100  $\mu\text{M}$ ) significantly reduced the ATP $\gamma\text{S}$ -mediated inhibition of PS amplitude (Fig. 5b) and completely prevented the potentiation of the stimulus-response curve (data not shown). As observed at the dendritic level, the effect of ATP $\gamma\text{S}$  on PS amplitude was completely antagonized by the adenosine  $\text{A}_1$  selective antagonist, DPCPX (Fig. 5b).



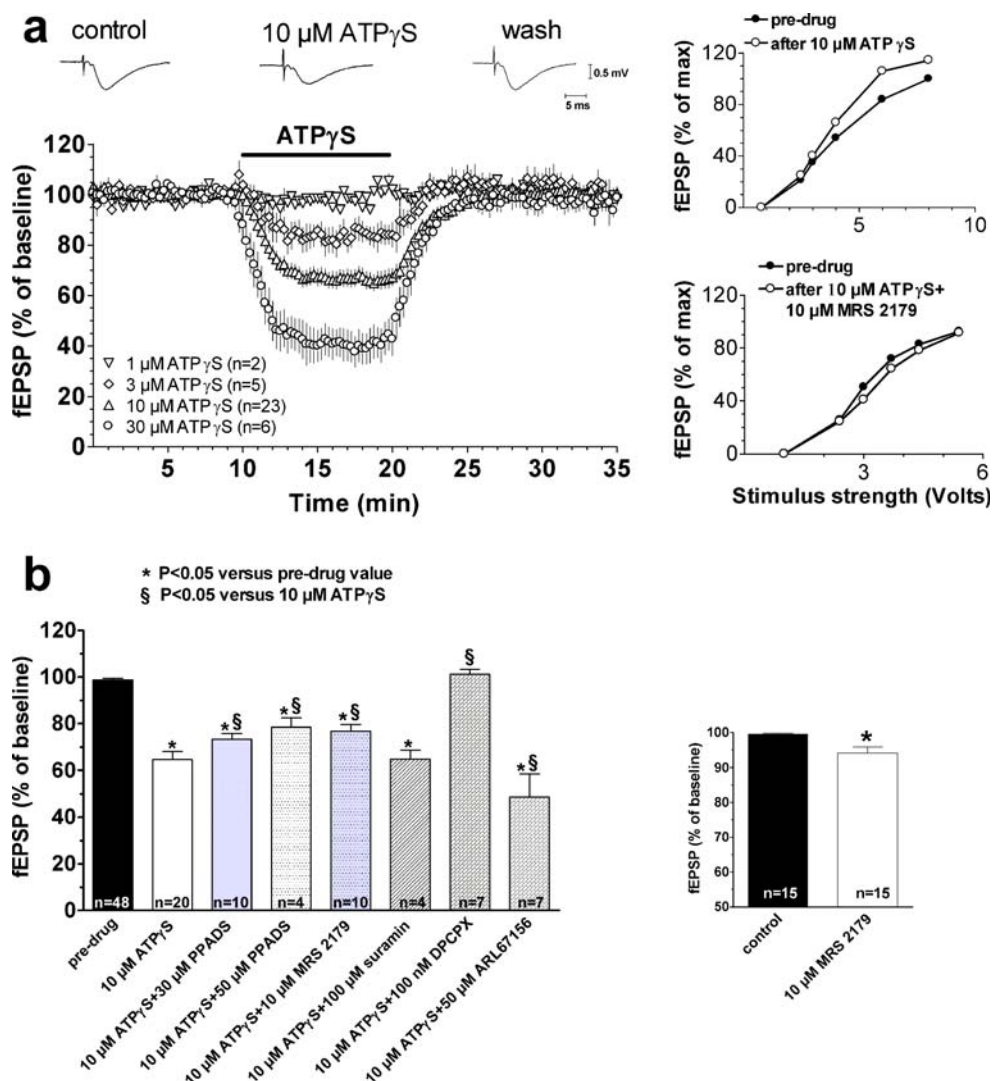


**Fig. 4** The inhibitory effect induced by ATP $\gamma\text{S}$  on fEPSP amplitude is reduced by the P2 purinergic antagonists PPADS and MRS 2179 and is enhanced by the ecto-ATPase inhibitor ARL 67156. **a** Time course of fEPSP amplitude before, during and after the application of different concentrations of ATP $\gamma\text{S}$ . Each point in the graph represents the mean  $\pm$  SE of the fEPSP value measured as percent of baseline, pre-drug level. Note that the P2 agonist was ineffective at 1  $\mu\text{M}$  whereas a significant inhibition of fEPSP amplitude was observed starting from a concentration of 3  $\mu\text{M}$  ( $P < 0.05$ , paired Student's  $t$ -test). *Upper panels* represent single traces recorded in a typical experiment before, during and after 10  $\mu\text{M}$  ATP $\gamma\text{S}$  application. *Upper inset*: stimulus-response curves recorded before and after 10  $\mu\text{M}$  ATP $\gamma\text{S}$  application illustrate the potentiating effect of the P2 agonist on a wide range of stimulus strengths in a typical experiment. fEPSP amplitude is expressed as percent of the maximal value obtained under control conditions at the highest stimulus strength. Note the increase in fEPSP amplitude recorded 15 min after 10  $\mu\text{M}$  ATP $\gamma\text{S}$  removal at stimulus intensities

able to evoke more than 50% of the maximal response. *Lower inset*: the potentiating effect was prevented in the presence of 10  $\mu\text{M}$  MRS 2179. **b** *Columns* in the graph summarize the average amplitude (mean  $\pm$  SE) of evoked fEPSP recorded from hippocampal slices under control conditions, 5 min after superfusion of ATP $\gamma\text{S}$  alone and 5 min after ATP $\gamma\text{S}$  superfusion in the presence of different drugs. Note that the inhibitory effect of ATP $\gamma\text{S}$  on fEPSP amplitude is antagonized by the P2 antagonists PPADS and MRS 2179, but not by suramin. The A<sub>1</sub> adenosine antagonist DPCPX blocked the effect induced by 10  $\mu\text{M}$  ATP $\gamma\text{S}$ . In the presence of ARL 67156 the inhibitory effect of ATP $\gamma\text{S}$  was increased. \* $P < 0.05$ , one-way ANOVA followed by Newman-Keuls test versus pre-drug value.  $\S P < 0.05$ , one-way ANOVA followed by Newman-Keuls test versus 10  $\mu\text{M}$  ATP $\gamma\text{S}$ -treated slices. *Inset*: *bars* in the graph represent the average of fEPSP amplitude recorded 5 min before and during the last 5 min of 10  $\mu\text{M}$  MRS 2179 application. A significant difference was found between the two values (\* $P < 0.05$ , paired Student's  $t$ -test)

Figure 6 shows the concentration-response curves obtained for ATP and ATP $\gamma\text{S}$  at both the dendritic and somatic levels. It can be noted that lower concentrations of both P2 agonists are necessary to elicit the inhibitory effect

on PS amplitude in comparison to what is observed at the dendritic level. In addition, the figure shows that ATP $\gamma\text{S}$  is more efficient in reducing fEPSP amplitude (but not PS amplitude) in comparison to ATP.

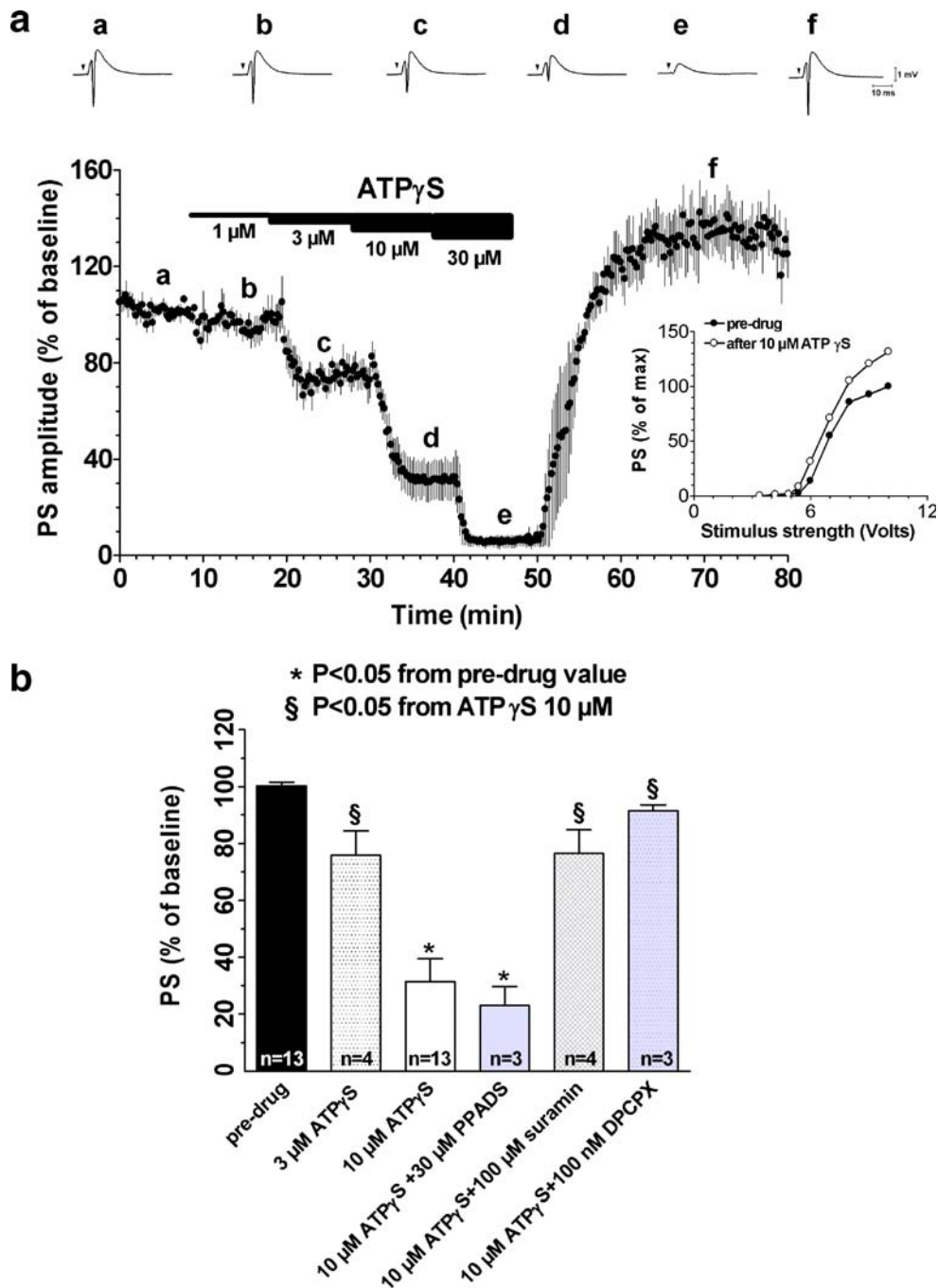


**Fig. 5** ATP $\gamma$ S induces a concentration-dependent inhibition and a subsequent potentiation of PS amplitude in the CA1 region of rat hippocampus. **a** Time course of PS amplitude before, during and after the application of different concentrations of ATP $\gamma$ S. Each point in the graph represents the mean  $\pm$  SE of the PS value measured as percent of baseline, pre-drug level. Note that the P2 agonist was ineffective at 1  $\mu$ M, whereas a significant inhibition of fEPSP amplitude was observed starting from a concentration of 3  $\mu$ M ( $P < 0.05$ , paired Student's  $t$ -test). Note the persistent increase in synaptic potential amplitude after drug removal. The bar indicates the time duration of ATP $\gamma$ S application. Upper panels represent single traces recorded in a typical experiment before, during and after ATP $\gamma$ S application (10  $\mu$ M). Inset: stimulus-response curve recorded before and after 10  $\mu$ M ATP $\gamma$ S application illustrate the potentiating effect of the P2 agonist on a wide range of stimulus strengths in a typical

experiment. PS amplitude is expressed as percent of the maximal value obtained under control conditions at the highest stimulus strength. Note the increase in PS amplitude recorded 15 min after 10  $\mu$ M ATP $\gamma$ S removal at stimulus intensities able to evoke more than 20% of the maximal amplitude (mean  $\pm$  SE) of evoked PS recorded from hippocampal slices under control conditions, 5 min after superfusion of ATP $\gamma$ S alone and 5 min after ATP $\gamma$ S superfusion in the presence of different purinergic antagonists. Note that the inhibitory effect of ATP $\gamma$ S on PS amplitude is not antagonized by the P2 antagonists PPADS, is reduced by the P2 antagonist suramin and is blocked by the A<sub>1</sub> adenosine antagonist DPCPX. \* $P < 0.05$ , one-way ANOVA followed by Newman-Keuls test versus respective pre-drug value. § $P < 0.05$ , one-way ANOVA followed by Newman-Keuls test versus 10  $\mu$ M ATP $\gamma$ S-treated slices

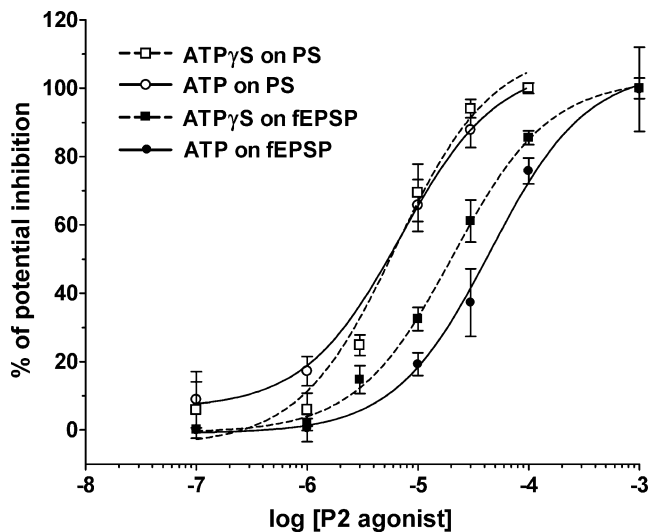


**Fig. 6** Concentration-response curves of ATP and ATP $\gamma$ S on dendritic fEPSP and somatic PS responses. The graph shows the fitting curves of concentration-dependent inhibitory effects of ATP and ATP $\gamma$ S on fEPSP and PS amplitude. Note that the curves obtained for both purinergic agonists at the somatic level are shifted to the left in respect to those recorded at the dendritic level. In addition, at the dendritic level, the concentration-response curve obtained in the presence of ATP $\gamma$ S is steeper than that obtained in the presence of ATP

#### Effects of ATP and ATP $\gamma$ S on PPF in the CA1 region of the rat hippocampus

In order to discern if the ATP- and ATP $\gamma$ S-mediated effects on fEPSP amplitude were due to pre- or postsynaptic mechanisms, we performed a PPF protocol (see “Methods”). As shown in Table 1, a 10-min application of 10  $\mu$ M ATP increased PPF, an effect that is not statistically significant. On the other hand, at a concentration of 100  $\mu$ M, a significant increase in PPF was observed ( $P < 0.01$ , paired Student’s *t*-test). Ten minutes application of ATP $\gamma$ S significantly increased PPF starting from a concentration of 10  $\mu$ M (Table 1).

To clarify if these effects on PPF were due to P1 or P2 receptor activation, we tested different purinergic antagonists. The action elicited by ATP was tested only in the presence of DPCPX, since we previously demonstrated that PPADS and suramin are not able to antagonize the ATP-inhibitory effect on fEPSP amplitude.

DPCPX (100 nM) alone decreased PPF and fully prevented the ATP-mediated effect. Since the effects of ATP $\gamma$ S at the dendritic level were blocked by both P2 and the A<sub>1</sub> receptor antagonists, the effect was checked in the presence of PPADS, MRS 2179 and DPCPX.

PPADS (30  $\mu$ M) and MRS 2179 (10  $\mu$ M), applied alone, 10 and 15 min before agonist superfusion, respectively, significantly increased, *per se*, the P2/P1 ratio, but failed to block the increase in PPF induced by 10  $\mu$ M ATP $\gamma$ S. DPCPX (100 nM) alone decreased PPF and fully prevented the ATP $\gamma$ S-mediated effect (Table 1).

#### Effects of different purinergic antagonists on OGD-evoked disruption of neurotransmission in the CA1 region of rat hippocampal slices

The role of P2 purinergic receptor stimulation by endogenous ATP released during *in vitro* OGD episodes on the impairment of synaptic transmission was investigated using P2-selective antagonists.

In a first series of experiments we characterized the synaptic response of evoked fEPSPs following severe (7 min) OGD, an ischaemia-like insult that under our experimental conditions has been constantly shown to produce an irreversible loss of synaptic transmission [52, 53]. At the same time as the fEPSPs recordings, we also monitored another important parameter of brain tissue integrity, the DC shift produced by AD. It is well described in the literature that AD is one of the major factors inducing brain damage after an ischaemic episode [77].

**Table 1** Effects of P2 purinergic agonists and antagonists on paired-pulse facilitation in the CA1 hippocampal region

	<i>n</i>	P2/P1 ratio		<i>n</i>	P2/P1 ratio
Pre-drug	2	1.49±0.12	Pre-drug	5	1.31±0.01
10 $\mu$ M ATP	2	1.59±0.13	100 nM DPCPX	5	1.29±0.05*
Wash	2	1.48±0.11	100 nM DPCPX + 100 $\mu$ M ATP	5	1.29±0.04
Pre-drug	5	1.54±0.06	Pre-drug	4	1.32±0.02
100 $\mu$ M ATP	5	2.16±0.06*	100 nM DPCPX	4	1.25±0.07*
Wash	5	1.56±0.06	100 nM DPCPX + 10 $\mu$ M ATP $\gamma$ S	4	1.22±0.07
Pre-drug	9	1.48±0.08	Pre-drug	6	1.51±0.08
10 $\mu$ M ATP $\gamma$ S	9	1.69±0.06*	30 $\mu$ M PPADS	6	1.53±0.09*
Wash	8	1.47±0.09	30 $\mu$ M PPADS + 10 $\mu$ M ATP $\gamma$ S	6	1.90±0.12**
Pre-drug	4	1.49±0.03	Pre-drug	8	1.43±0.04
30 $\mu$ M ATP $\gamma$ S	4	1.90±0.07*	10 $\mu$ M MRS	8	1.46±0.04*
Wash	4	1.50±0.03	10 $\mu$ M MRS + 10 $\mu$ M ATP $\gamma$ S	8	1.67±0.08**

\* $P < 0.05$  from respective pre-drug value (paired Student’s *t*-test)

\*\* $P < 0.05$  from antagonist alone (paired Student’s *t*-test)

One 7-min OGD episode induced the disappearance of fEPSP, which did not recover ( $4.2 \pm 1.9\%$ ,  $n=13$ ) after superfusion with oxygenated, glucose-containing aCSF as monitored up to 80 min. In addition, in all control slices, AD was recorded as a DC shift with a mean peak latency of  $6.2 \pm 0.2$  min after OGD initiation and a mean peak amplitude of  $6.1 \pm 0.6$  mV (Table 2).

In the presence of PPADS, a non-selective P2 antagonist, the irreversible block of synaptic transmission induced by 7-min OGD was prevented in five of the six slices tested. As shown in Fig. 7a (open circles), 30  $\mu$ M PPADS, applied 10 min before, during and 5 min after the OGD insult, allowed a significant recovery of fEPSP amplitude within 15-min reperfusion with oxygenated and glucose-containing aCSF (from  $4.2 \pm 2.1\%$  of fEPSP recovery in control slices to  $79 \pm 16.6\%$  in the presence of 30  $\mu$ M PPADS,  $n=6$ ). Figure 7b shows that in this experimental group, only three of six slices exposed to 7-min OGD presented a sizeable AD ( $>1$  mV) whose peak latency was delayed ( $7.1 \pm 1$  min) by PPADS 30  $\mu$ M. One of these three slices, in spite of the appearance of AD (2.5 mV, 30 s after oxygen and glucose restoration) recovered a significant fraction (78.5%) of original fEPSP amplitude after 20 min of reperfusion.

As shown in Table 2, similar results were obtained in the presence of different purinergic antagonists: suramin, MRS 2179 and BBG. In all cases the effect on recovery of fEPSP amplitude (Fig. 7c) and AD inhibition was concentration-dependent. In addition, in 8 of all 29 slices treated with the P2 antagonists, no AD appearance was observed. In the remaining 21 treated slices in which AD was recorded, its appearance was significantly delayed ( $7.1 \pm 0.2$  min after OGD initiation). A significant recovery of fEPSP amplitude ( $>15\%$  of preischaeamic value) was observed in 10 of the 21 treated slices in which AD emerged.

## Discussion

### Role of P2 receptors in hippocampal neurotransmission under normoxic conditions

Our results demonstrate that ATP or its stable analogue ATP $\gamma$ S modulate evoked synaptic transmission in the CA1 region of the rat hippocampus. The main effect, observed within the first 2–3 min of drug application, is a reduction in fEPSP and PS amplitude evoked by electrical stimulation of the Schaffer collateral-commissural pathway. This effect is concentration dependent and reversible after a few minutes of washout. Another effect elicited by both ATP and ATP $\gamma$ S is a significant potentiation of evoked responses, recorded after drug removal and persisting for at least 30 min.

The inhibitory effect observed during ATP application has already been described and attributed to P1 [32–34] or to P2 receptor stimulation [35, 36].

Our observation that the selective A<sub>1</sub> receptor antagonist DPCPX blocks ATP-induced inhibition of synaptic responses indicates that adenosine formed from ATP catabolism and acting at A<sub>1</sub> receptors is responsible for synaptic depression. We would therefore expect that the ecto-ATPase inhibitors tested (ARL 67156, BGO 136 and PV4) antagonize the ATP inhibition of synaptic responses. On the contrary, all the ecto-ATPase inhibitors potentiate the ATP inhibitory effect, suggesting that they unmask a significant ATP-mediated inhibitory action that is otherwise covered by adenosine acting on A<sub>1</sub> receptors. This interpretation is supported by the observation that both ATP- and ATP $\gamma$ S-mediated inhibitory responses are partially blocked by the unselective P2 antagonists suramin and PPADS and the selective P2Y<sub>1</sub> antagonist MRS 2179. These observations indicate that, in addition to P1 receptor activation, a P2 component is

**Table 2** Effects of P2 purinergic receptor antagonists on CA1 hippocampal synaptic transmission after 7 min of OGD<sup>a</sup>

		AD appearance ( <i>n/n</i> )	AD peak time (min)	AD peak amplitude (mV)	fEPSP recovery $\geq$ 15% ( <i>n/n</i> )	fEPSP recovery (%) after 15 min reperfusion
Control	$n=13$	(13/13)	$6.2 \pm 0.2$	$6.1 \pm 0.6$	(0/13)	$4.2 \pm 1.9$
PPADS	10 $\mu$ M ( $n=4$ )	(3/4)	$6.4 \pm 0.3$	$6.2 \pm 0.3$	(3/4)	$34.3 \pm 18.7$
	30 $\mu$ M ( $n=6$ )	(3/6)	$7.1 \pm 0.9$	$5.9 \pm 0.4$	(5/6)	$65.9 \pm 20^*$
MRS 2179	1 $\mu$ M ( $n=3$ )	(2/3)	$7.5 \pm 0.6$	$6.8 \pm 1.8$	(2/3)	$42.9 \pm 29.7$
	10 $\mu$ M ( $n=5$ )	(2/5)	$7 \pm 0.3$	$4 \pm 1.8$	(4/5)	$79.2 \pm 18.2^*$
Suramin	10 $\mu$ M ( $n=4$ )	(3/4)	$7.6 \pm 0.6$	$6 \pm 2.3$	(2/4)	$53.1 \pm 29.5$
	100 $\mu$ M ( $n=3$ )	(2/3)	$6.6 \pm 0.5$	$4.7 \pm 1.1$	(3/3)	$80.5 \pm 11.9^*$
BBG	500 nM ( $n=4$ )	(2/4)	$6.1 \pm 0.3$	$7.9 \pm 0.4$	(2/4)	$57.6 \pm 31.6$
	1 $\mu$ M ( $n=7$ )	(4/7)	$7.9 \pm 0.3$	$6.7 \pm 0.8$	(4/7)	$52.9 \pm 16.3^*$

<sup>a</sup> Data are taken from slices receiving 7-min OGD under control conditions or in the presence of different P2 purinergic antagonists. Numbers in parentheses (*n/n*) indicate the number of observations out of investigated slices. Time is calculated from OGD initiation. The amplitude of the final fEPSP recovery is expressed as percent of baseline fEPSP value recorded 5 min before OGD application. \* $P < 0.01$  from control value (one-way ANOVA followed by Newman-Keuls test)

responsible for an ATP-mediated decrease in synaptic transmission in the CA1 area of the rat hippocampus.

The block of ATP $\gamma$ S effect by DPCPX is unexpected because the agonist is considered a metabolically stable ATP analogue. Our result is however in support of previous observations that at least a fraction of ATP $\gamma$ S undergoes enzymatic degradation and activates A<sub>1</sub> adenosine receptors [34]. An enzymatic degradation of ATP $\gamma$ S is further supported by the result that ARL 67156 potentiates the inhibitory effect of this P2 agonist.

It has been suggested that, in hippocampal neurones, ATP may activate DPCPX-sensitive P2 receptors [35]. The existence of a heteromeric association between A<sub>1</sub> and P2Y<sub>1</sub> receptors was demonstrated by co-localization staining, co-immunoprecipitation and bioluminescence resonance energy transfer technology in HEK293T cells transfected with both A<sub>1</sub> and P2Y<sub>1</sub> receptors [78, 79] and in primary cultures of cortical, hippocampal and cerebellar neurones [80]. Therefore, we could hypothesize that DPCPX sensitivity of both ATP and ATP $\gamma$ S inhibitory effects is attributable both to their enzymatic degradation to adenosine and to the activation of the heteromeric A<sub>1</sub>-P2Y<sub>1</sub> receptor. The fact that, in the present work, the P2Y<sub>1</sub> antagonist MRS 2179 reduces the ATP $\gamma$ S-inhibitory effect on fEPSP amplitude supports this notion.

Other groups have previously described a persistent ATP-induced potentiation of CA1 hippocampal neurotransmission [41, 71–76]. We clearly observed this phenomenon after a prolonged application of ATP $\gamma$ S during somatic recordings. When the dendritic potential was measured, the increase in fEPSP amplitude elicited by both purinergic agonists was detectable only by evoking a stimulus-response curve 15 min after drug removal. The increase in fEPSP amplitude was statistically significant only at the highest stimulus intensities tested. The potentiating effect elicited by ATP and ATP $\gamma$ S application is completely blocked by P2 antagonists at both the dendritic and somatic levels, demonstrating that it is due to P2 receptor stimulation. It has to be noted that higher stimulus strengths are needed to observe a potentiation of dendritic potentials in comparison to somatic responses and that ATP and ATP $\gamma$ S induce a significant potentiation of PS amplitude at lower concentrations in respect to those required at the dendritic level. Altogether, these data suggest that both presynaptic P2 receptors modulating glutamate release and postsynaptic P2 receptors modulating cell excitability are involved in potentiation of CA1 hippocampal neurotransmission. The P2 antagonists PPADS and MRS 2179 applied alone significantly decrease fEPSP amplitude. At the somatic level, only suramin diminishes the evoked responses. These observations demonstrate that in the CA1 region of rat hippocampal slices there is an endogenous tonic activation of P2 receptors that contributes to excitatory

neurotransmission and is in agreement with those reported in the rat hippocampus [21, 43] and prefrontal cortex [36, 30]. The varying efficacy of the P2 antagonists at the dendritic and somatic levels suggests that different subtypes of P2 receptors located in the pre- and postsynaptic compartment are involved in the excitatory effect.

The role of P2 agonist application was also evaluated by using a PPF protocol. The P2/P1 ratio was significantly increased by ATP and ATP $\gamma$ S application. The same effect has been described in hippocampal slices during exogenous adenosine application by other groups [81] and is attributed to an adenosine A<sub>1</sub> receptor-mediated decrease of glutamate release. Our data indicate that the increase in PPF elicited by ATP application is completely blocked by DPCPX, suggesting that it is effectively due to A<sub>1</sub> receptor stimulation after ATP conversion to adenosine. Similar results are observed for ATP $\gamma$ S-induced PPF increase, because it is not blocked by PPADS or MRS 2179, but only by DPCPX. These data support the hypothesis that part of ATP $\gamma$ S is converted to adenosine and activates A<sub>1</sub> receptors. It should be noted that both purinergic antagonists (PPADS and MRS 2179) applied alone induced a significant increase of PPF (P2/P1 ratio). This observation indicates that ATP contributes to excitatory neurotransmission stimulating the release of glutamate. These results are in line with those obtained by Rodrigues et al. [17] on hippocampal synaptosomes.

#### Role of P2 receptors in hippocampal neurotransmission during OGD

The application of purinergic antagonists before, during and after a severe (7 min) OGD insult allows a significant recovery of fEPSP amplitude that is never observed in control slices. The concentration range of the drug effects falls within the  $K_i$  value estimated for all the antagonists in the rat tissue [1, 65].

The mechanism by which these drugs protect hippocampal slices from the OGD-induced irreversible loss of synaptic transmission is likely correlated to AD appearance [53], a phenomenon that contributes to cell damage during ischaemia (for a review: see [77]). In fact, in all 13 control slices, AD is recorded within the 7-min OGD insult (mean latency of AD appearance: 6.2±0.2 min after OGD initiation) and the recovery of fEPSP amplitude after 15 min of reperfusion in oxygenated and glucose-containing aCSF is always less than 10% of the preischaemic value. On the contrary, P2 antagonists both delay or block AD appearance and allow a significant recovery of neurotransmission.

Our data suggest that hippocampal P2 receptors activated during OGD by endogenously released ATP exert a deleterious role on CA1 neurotransmission by participating in AD appearance.

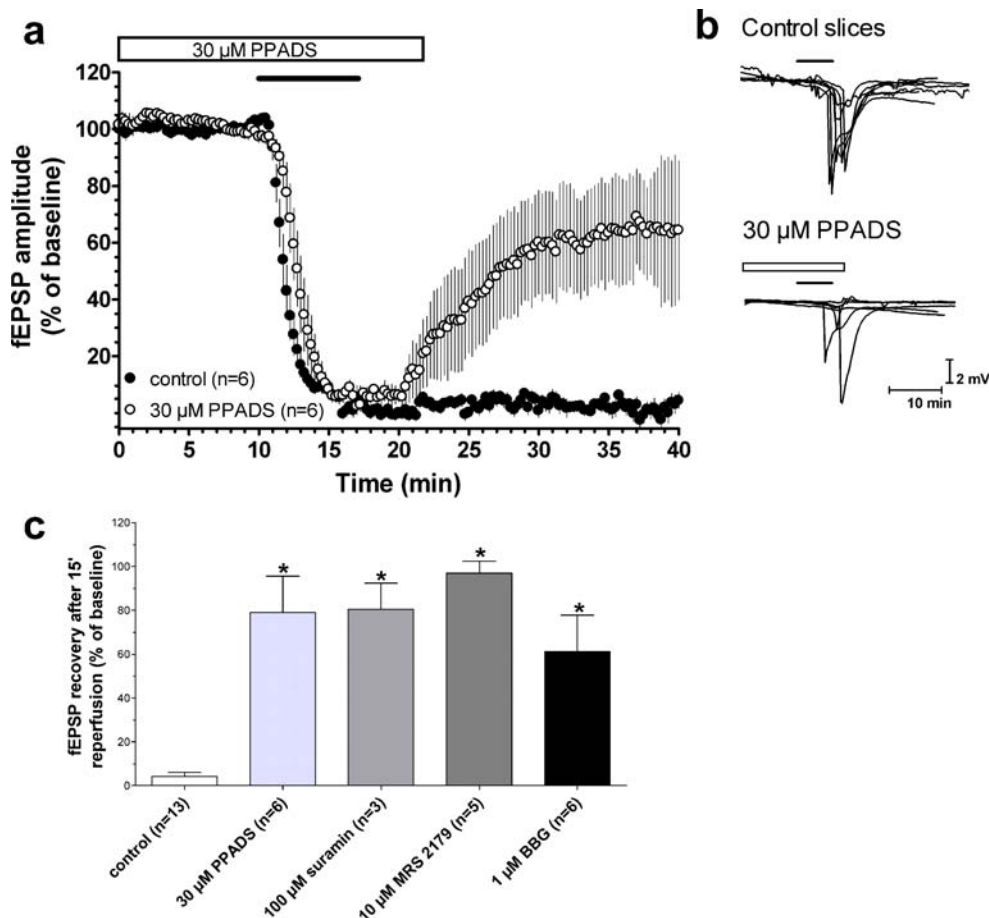


**Fig. 7** Different purinergic antagonists are able to prevent the irreversible loss of hippocampal CA1 neurotransmission after 7-min OGD. **a** The graph shows the time courses of fEPSP amplitude before, during 7 min of OGD and after reperfusion in normal oxygenated aCSF in the absence and in the presence of 30 μM PPADS (open bar), a P2 unselective receptor antagonist. Data (mean ± SE) are expressed as a percent of the baseline values. **b** In the same groups of slices, AD was recorded as a negative voltage shift in response to 7 min of OGD in control slices (upper panel) and in the presence of 30 μM PPADS (lower panel). Note that PPADS blocked AD appearance in three of

six slices and delayed the latency in the remaining three slices. *Solid bars* indicate the time duration of OGD. **c** Columns in the graph summarize the average recovery (mean ± SE) of fEPSP amplitude in CA1 hippocampal slices after 7 min of OGD under control conditions or in the presence of different P2 purinergic antagonists. Only slices showing a fEPSP recovery >15% after 15 min of reperfusion were included in the analysis. Note that all drugs allow a significant recovery of fEPSP amplitude after 7 min of OGD. \* $P < 0.001$ , one-way ANOVA, followed by Newman-Keuls test versus control, untreated slices

An increase in extracellular ATP concentration during ischaemia was demonstrated in hippocampal slices by Juranyi et al. [44] and Frenguelli et al. [82] who report a peak in extracellular ATP concentration immediately before AD appearance during an OGD insult. In agreement with our results, the same authors show that this phenomenon is always followed by the complete loss of synaptic transmission.

Under ischaemic conditions both direct and indirect actions could account for P2 receptor antagonist-mediated protection. A protective effect of P2 antagonists may be attributed to a direct inhibition of  $\text{Ca}^{2+}$  intracellular loading in neuronal and glial cells [83, 84]. In fact, calcium is a main toxicity factor under ischaemia [85]. Further possible indirect protective effects of P2 receptor antagonists may reside in the prevention of glutamate-evoked toxicity [86, 87] and in maintaining normal energetic stores [88].

Antagonism of P2 receptors during ischaemia might also regulate intracellular pathways involved in ischaemia-associated necrosis/apoptosis pathways such as expression of the glucose-regulated protein GRP75 and of the caspase-2 enzyme [89].

Among the antagonists checked in the present model, the high selectivity of BBG indicates that  $\text{P2X}_7$  receptors are clearly involved in the deleterious effects induced by OGD in the CA1 hippocampal region. In addition, the participation of  $\text{P2Y}_1$  receptors in this effect is supported by the efficacy of MRS 2179 in blocking AD appearance and preventing the irreversible loss of neurotransmission induced by a severe OGD.

These results are in agreement with the protective effect exerted by P2 antagonists in *in vitro* OGD [50, 51] and *in vivo* ischaemic conditions [47–49].

## Conclusions

We conclude that P2 receptors play an important role in CA1 hippocampal neurotransmission under both normoxic and ischaemic conditions. Under normoxic conditions, both inhibitory and excitatory effects are observed after application of ATP or the stable analogue ATP $\gamma$ S. The inhibition of CA1 neurotransmission recorded during ATP application, under our experimental conditions, is mostly due to the enzymatic degradation to adenosine and subsequent activation of A<sub>1</sub> receptors. The ATP analogue ATP $\gamma$ S evokes an inhibition of hippocampal neurotransmission by both P2 and A<sub>1</sub> adenosine receptors. A later excitatory effect, as pointed out by enhancement of fEPSP and PS amplitude, is attributable only to P2 receptors. In addition, a tonic activation of P2 receptors (likely located at a presynaptic level since their block enhances PPF) contributes to the excitatory neurotransmission normally recorded in this brain area.

Under *in vitro* ischaemic conditions (OGD), a deleterious role of ATP is suggested by the observation that P2 antagonists allow the restoration of neurotransmission after an otherwise lethal insult and block or delay the appearance of AD.

**Acknowledgements** The present work was supported by: University of Florence (60%); FIRB (RBAU019ZEN\_004), PRIN-COFIN and “Ente Cassa Di Risparmio” of Florence, Italy (2006/40600).

## References

- Ralevic V, Burnstock G (1998) Receptors for purines and pyrimidines. *Pharmacol Rev* 50(3):413–492
- Wieraszko A, Goldsmith G, Seyfried TN (1989) Stimulation-dependent release of adenosine triphosphate from hippocampal slices. *Brain Res* 485(2):244–250
- Mori M, Heuss C, Gahwiler BH, Gerber U (2001) Fast synaptic transmission mediated by P2X receptors in CA3 pyramidal cells of rat hippocampal slice cultures. *J Physiol* 535(Pt 1):115–123
- Khakh BS, Henderson G (1998) ATP receptor-mediated enhancement of fast excitatory neurotransmitter release in the brain. *Mol Pharmacol* 54(2):372–378
- Koizumi S, Fujishita K, Tsuda M, Shigemoto-Mogami Y, Inoue K (2003) Dynamic inhibition of excitatory synaptic transmission by astrocyte-derived ATP in hippocampal cultures. *Proc Natl Acad Sci U S A* 100(19):11023–11028
- Zhang JM, Wang HK, Ye CQ, Ge W, Chen Y, Jiang ZL, Wu CP, Poo MM, Duan S (2003) ATP released by astrocytes mediates glutamatergic activity-dependent heterosynaptic suppression. *Neuron* 40(5):971–982
- Sperlgh B, Magloczky Z, Vizi ES, Freund TF (1998) The triangular septal nucleus as the major source of ATP release in the rat habenula: a combined neurochemical and morphological study. *Neuroscience* 86(4):1195–1207
- Abbracchio MP, Burnstock G (1994) Purinoceptors: are there families of P2X and P2Y purinoceptors? *Pharmacol Ther* 64(3):445–475
- Collo G, North RA, Kawashima E, Merlo-Pich E, Neidhart S, Surprenant A, Buell G (1996) Cloning OF P2X5 and P2X6 receptors and the distribution and properties of an extended family of ATP-gated ion channels. *J Neurosci* 16(8):2495–2507
- Inoue K, Koizumi S, Ueno S (1996) Implication of ATP receptors in brain functions. *Prog Neurobiol* 50(5–6):483–492
- Khakh BS (2001) Molecular physiology of P2X receptors and ATP signalling at synapses. *Nat Rev Neurosci* 2(3):165–174
- North RA (2002) Molecular physiology of P2X receptors. *Physiol Rev* 82(4):1013–1067
- von Kugelgen I, Wetter A (2000) Molecular pharmacology of P2Y-receptors. *Naunyn Schmiedebergs Arch Pharmacol* 362(4–5):310–323
- Ciana P, Fumagalli M, Trincavelli ML, Verderio C, Rosa P, Lecca D, Ferrario S, Parravicini C, Capra V, Gelosa P, Guerrini U, Belcredito S, Cimino M, Sironi L, Tremoli E, Rovati GE, Martini C, Abbracchio MP (2006) The orphan receptor GPR17 identified as a new dual uracil nucleotides/cysteinyll-leukotrienes receptor. *EMBO J* 25(19):4615–4627
- Lazarowski ER, Boucher RC, Harden TK (2003) Mechanisms of release of nucleotides and integration of their action as P2X- and P2Y-receptor activating molecules. *Mol Pharmacol* 64(4):785–795
- Rubio ME, Soto F (2001) Distinct Localization of P2X receptors at excitatory postsynaptic specializations. *J Neurosci* 21(2):641–653
- Rodrigues RJ, Almeida T, Richardson PJ, Oliveira CR, Cunha RA (2005) Dual presynaptic control by ATP of glutamate release via facilitatory P2X1, P2X2/3, and P2X3 and inhibitory P2Y1, P2Y2, and/or P2Y4 receptors in the rat hippocampus. *J Neurosci* 25(27):6286–6295
- Hugel S, Schlichter R (2000) Presynaptic P2X receptors facilitate inhibitory GABAergic transmission between cultured rat spinal cord dorsal horn neurons. *J Neurosci* 20(6):2121–2130
- Nakatsuka T, Gu JG (2001) ATP P2X receptor-mediated enhancement of glutamate release and evoked EPSCs in dorsal horn neurons of the rat spinal cord. *J Neurosci* 21(17):6522–6531
- Cunha RA, Ribeiro JA (2000) ATP as a presynaptic modulator. *Life Sci* 68(2):119–137
- Pankratov Y, Castro E, Miras-Portugal MT, Krishtal O (1998) A purinergic component of the excitatory postsynaptic current mediated by P2X receptors in the CA1 neurons of the rat hippocampus. *Eur J Neurosci* 10(12):3898–3902
- Pankratov Y, Lalo U, Krishtal O, Verkhratsky A (2002) Ionotropic P2X purinoceptors mediate synaptic transmission in rat pyramidal neurones of layer II/III of somato-sensory cortex. *J Physiol* 542(Pt 2):529–536
- Edwards FA, Gibb AJ, Colquhoun D (1992) ATP receptor-mediated synaptic currents in the central nervous system. *Nature* 359(6391):144–147
- Nieber K, Poelchen W, Illes P (1997) Role of ATP in fast excitatory synaptic potentials in locus coeruleus neurones of the rat. *Br J Pharmacol* 122(3):423–430
- Khakh BS, Humphrey PP, Henderson G (1997) ATP-gated cation channels (P2X purinoceptors) in trigeminal mesencephalic nucleus neurons of the rat. *J Physiol* 498 (Pt 3):709–715
- Inoue K, Nakazawa K, Fujimori K, Watano T, Takanaka A (1992) Extracellular adenosine 5'-triphosphate-evoked glutamate release in cultured hippocampal neurons. *Neurosci Lett* 134(2):215–218
- Aihara H, Fujiwara S, Mizuta I, Tada H, Kanno T, Tozaki H, Nagai K, Yajima Y, Inoue K, Kondoh T, Motooka Y, Nishizaki T (2002) Adenosine triphosphate accelerates recovery from hypoxic/hypoglycemic perturbation of guinea pig hippocampal neurotransmission via a P(2) receptor. *Brain Res* 952(1):31–37
- Armstrong JN, Brust TB, Lewis RG, MacVicar BA (2002) Activation of presynaptic P2X7-like receptors depresses mossy fiber-CA3 synaptic transmission through p38 mitogen-activated protein kinase. *J Neurosci* 22(14):5938–5945

29. Kawamura M, Gachet C, Inoue K, Kato F (2004) Direct excitation of inhibitory interneurons by extracellular ATP mediated by P2Y1 receptors in the hippocampal slice. *J Neurosci* 24(48):10835–10845
30. Wirkner K, Koles L, Thummler S, Luthardt J, Poelchen W, Franke H, Furst S, Illes P (2002) Interaction between P2Y and NMDA receptors in layer V pyramidal neurons of the rat prefrontal cortex. *Neuropharmacology* 42(4):476–488
31. Koizumi S, Inoue K (1997) Inhibition by ATP of calcium oscillations in rat cultured hippocampal neurones. *Br J Pharmacol* 122(1):51–58
32. Dunwiddie TV, Diao L, Proctor WR (1997) Adenine nucleotides undergo rapid, quantitative conversion to adenosine in the extracellular space in rat hippocampus. *J Neurosci* 17(20):7673–7682
33. Cunha RA, Sebastiao AM, Ribeiro JA (1998) Inhibition by ATP of hippocampal synaptic transmission requires localized extracellular catabolism by ecto-nucleotidases into adenosine and channeling to adenosine A1 receptors. *J Neurosci* 18(6):1987–1995
34. Masino SA, Diao L, Illes P, Zahniser NR, Larson GA, Johansson B, Fredholm BB, Dunwiddie TV (2002) Modulation of hippocampal glutamatergic transmission by ATP is dependent on adenosine a(1) receptors. *J Pharmacol Exp Ther* 303(1):356–363
35. Mendoza-Fernandez V, Andrew RD, Barajas-Lopez C (2000) ATP inhibits glutamate synaptic release by acting at P2Y receptors in pyramidal neurons of hippocampal slices. *J Pharmacol Exp Ther* 293(1):172–179
36. Luthardt J, Borvendeg SJ, Sperlagh B, Poelchen W, Wirkner K, Illes P (2003) P2Y(1) receptor activation inhibits NMDA receptor-channels in layer V pyramidal neurons of the rat prefrontal and parietal cortex. *Neurochem Int* 42(2):161–172
37. Zimmermann H, Braun N (1996) Extracellular metabolism of nucleotides in the nervous system. *J Auton Pharmacol* 16(6):397–400
38. Fredholm BB, Chen JF, Masino SA, Vaugois JM (2005) Actions of adenosine at its receptors in the CNS: insights from knockouts and drugs. *Annu Rev Pharmacol Toxicol* 45:385–412
39. Latini S, Bordoni F, Corradetti R, Pepeu G, Pedata F (1999) Effect of A2A adenosine receptor stimulation and antagonism on synaptic depression induced by in vitro ischaemia in rat hippocampal slices. *Br J Pharmacol* 128(5):1035–1044
40. Latini S, Bordoni F, Pedata F, Corradetti R (1999) Extracellular adenosine concentrations during in vitro ischaemia in rat hippocampal slices. *Br J Pharmacol* 127(3):729–739
41. O’Kane EM, Stone TW (2000) Characterisation of ATP-induced facilitation of transmission in rat hippocampus. *Eur J Pharmacol* 409(2):159–166
42. Evans RJ, Derkach V, Surprenant A (1992) ATP mediates fast synaptic transmission in mammalian neurons. *Nature* 357(6378):503–505
43. Safiulina VF, Kasyanov AM, Sokolova E, Cherubini E, Giniatullin R (2005) ATP contributes to the generation of network-driven giant depolarizing potentials in the neonatal rat hippocampus. *J Physiol* 565(Pt 3):981–992
44. Juranyi Z, Sperlagh B, Vizi ES (1999) Involvement of P2 purinoceptors and the nitric oxide pathway in [3H]purine outflow evoked by short-term hypoxia and hypoglycemia in rat hippocampal slices. *Brain Res* 823(1–2):183–190
45. Melani A, Turchi D, Vannucchi MG, Cipriani S, Gianfriddo M, Pedata F (2005) ATP extracellular concentrations are increased in the rat striatum during in vivo ischemia. *Neurochem Int* 47(6):442–448
46. Ryu JK, Kim J, Choi SH, Oh YJ, Lee YB, Kim SU, Jin BK (2002) ATP-induced in vivo neurotoxicity in the rat striatum via P2 receptors. *Neuroreport* 13(13):1611–1615
47. Kharlamov A, Jones SC, Kim DK (2002) Suramin reduces infarct volume in a model of focal brain ischemia in rats. *Exp Brain Res* 147(3):353–359
48. Melani A, Amadio S, Gianfriddo M, Vannucchi MG, Volonte C, Bernardi G, Pedata F, Sancesario G (2006) P2X7 receptor modulation on microglial cells and reduction of brain infarct caused by middle cerebral artery occlusion in rat. *J Cereb Blood Flow Metab* 26(7):974–982
49. Lammer A, Gunther A, Beck A, Krugel U, Kittner H, Schneider D, Illes P, Franke H (2006) Neuroprotective effects of the P2 receptor antagonist PPADS on focal cerebral ischaemia-induced injury in rats. *Eur J Neurosci* 23(10):2824–2828
50. Cavaliere F, Florenzano F, Amadio S, Fusco FR, Viscomi MT, D’Ambrosi N, Vacca F, Sancesario G, Bernardi G, Molinari M, Volonte C (2003) Up-regulation of P2X2, P2X4 receptor and ischemic cell death: prevention by P2 antagonists. *Neuroscience* 120(1):85–98
51. Cavaliere F, Amadio S, Sancesario G, Bernardi G, Volonte C (2004) Synaptic P2X7 and oxygen/glucose deprivation in organotypic hippocampal cultures. *J Cereb Blood Flow Metab* 24(4):392–398
52. Pugliese AM, Latini S, Corradetti R, Pedata F (2003) Brief, repeated, oxygen-glucose deprivation episodes protect neurotransmission from a longer ischemic episode in the in vitro hippocampus: role of adenosine receptors. *Br J Pharmacol* 140(2):305–314
53. Pugliese AM, Coppi E, Spalluto G, Corradetti R, Pedata F (2006) A3 adenosine receptor antagonists delay irreversible synaptic failure caused by oxygen and glucose deprivation in the rat CA1 hippocampus in vitro. *Br J Pharmacol* 147(5):524–532
54. Zimmermann H (2000) Extracellular metabolism of ATP and other nucleotides. *Naunyn Schmiedebergs Arch Pharmacol* 362(4–5):299–309
55. Crack BE, Pollard CE, Beukers MW, Roberts SM, Hunt SF, Ingall AH, McKechnie KC, IJzerman AP, Leff P (1995) Pharmacological and biochemical analysis of FPL 67156, a novel, selective inhibitor of ecto-ATPase. *Br J Pharmacol* 114(2):475–481
56. Pascual O, Casper KB, Kubera C, Zhang J, Revilla-Sanchez R, Sul JY, Takano H, Moss SJ, McCarthy K, Hayden PG (2005) Astrocytic purinergic signaling coordinates synaptic networks. *Science* 310(5745):113–116
57. Iqbal J, Vollmayer P, Braun N, Zimmermann H, Muller CE (2005) A capillary electrophoresis method for the characterization of ecto-nucleoside triphosphate diphosphohydrolases (NTPDases) and the analysis of inhibitors by in-capillary enzymatic micro-reaction. *Purinergic Signalling* 1:349–358
58. Drakulich DA, Spellmon C, Hexum TD (2004) Effect of the ecto-ATPase inhibitor, ARL 67156, on the bovine chromaffin cell response to ATP. *Eur J Pharmacol* 485(1–3):137–140
59. Kukulski F, Komoszynski M (2003) Purification and characterization of NTPDase1 (ecto-apyrase) and NTPDase2 (ecto-ATPase) from porcine brain cortex synaptosomes. *Eur J Biochem* 270(16):3447–3454
60. Duval M, Beaudoin AR, Bkaily G, Gendron FP, Orleans-Juste P (2003) Characterization of the NTPDase activities in the mesentery pre- and post-capillary circuits of the guinea pig. *Can J Physiol Pharmacol* 81(3):212–219
61. Muller CE, Iqbal J, Baqi Y, Zimmermann H, Rollich A, Stephan H (2006) Polyoxometalates—a new class of potent ecto-nucleoside triphosphate diphosphohydrolase (NTPDase) inhibitors. *Bioorg Med Chem Lett* 16(23):5943–5947
62. Nakazawa K, Inoue K, Ito K, Koizumi S, Inoue K (1995) Inhibition by suramin and reactive blue 2 of GABA and glutamate receptor channels in rat hippocampal neurons. *Naunyn Schmiedebergs Arch Pharmacol* 351(2):202–208



63. Jiang LH, Mackenzie AB, North RA, Surprenant A (2000) Brilliant blue G selectively blocks ATP-gated rat P2X(7) receptors. *Mol Pharmacol* 58(1):82–88
64. Sperlagh B, Kofalvi A, Deuchars J, Atkinson L, Milligan CJ, Buckley NJ, Vizi ES (2002) Involvement of P2X7 receptors in the regulation of neurotransmitter release in the rat hippocampus. *J Neurochem* 81(6):1196–1211
65. Boyer JL, Mohanram A, Camaioni E, Jacobson KA, Harden TK (1998) Competitive and selective antagonism of P2Y1 receptors by N6-methyl 2'-deoxyadenosine 3',5'-bisphosphate. *Br J Pharmacol* 124(1):1–3
66. Camaioni E, Boyer JL, Mohanram A, Harden TK, Jacobson KA (1998) Deoxyadenosine bisphosphate derivatives as potent antagonists at P2Y1 receptors. *J Med Chem* 41(2):183–190
67. Charlton SJ, Brown CA, Weisman GA, Turner JT, Erb L, Boarder MR (1996) PPADS and suramin as antagonists at cloned P2Y- and P2U-purinoceptors. *Br J Pharmacol* 118(3):704–710
68. Moro S, Guo D, Camaioni E, Boyer JL, Harden TK, Jacobson KA (1998) Human P2Y1 receptor: molecular modeling and site-directed mutagenesis as tools to identify agonist and antagonist recognition sites. *J Med Chem* 41(9):1456–1466
69. Kraus W, Stephan H, Röllich A, Matejka Z, Reck G (2005)  $K_6H_2[TiW_{11}CoO_{40}] \cdot 13H_2O$ , with a titanoundecatungstocobaltate (II) anion. *Acta Cryst E* 61:i35–i37
70. Chen Y, Liu J (1997) Heteropoly complexes containing titanium. II. Synthesis and characterization of titanotungstocobaltates. *Synth React Inorg Metal-Org Chem* 27:239–250
71. Wieraszko A, Seyfried TN (1989) ATP-induced synaptic potentiation in hippocampal slices. *Brain Res* 491(2):356–359
72. Nishimura S, Mohri M, Okada Y, Mori M (1990) Excitatory and inhibitory effects of adenosine on the neurotransmission in the hippocampal slices of guinea pig. *Brain Res* 525(1):165–169
73. Fujii S, Kato H, Furuse H, Ito K, Osada H, Hamaguchi T, Kuroda Y (1995) The mechanism of ATP-induced long-term potentiation involves extracellular phosphorylation of membrane proteins in guinea-pig hippocampal CA1 neurons. *Neurosci Lett* 187(2):130–132
74. Fujii S, Kato H, Kuroda Y (1999) Extracellular adenosine 5'-triphosphate plus activation of glutamatergic receptors induces long-term potentiation in CA1 neurons of guinea pig hippocampal slices. *Neurosci Lett* 276(1):21–24
75. Fujii S, Kato H, Kuroda Y (2002) Cooperativity between extracellular adenosine 5'-triphosphate and activation of N-methyl-D-aspartate receptors in long-term potentiation induction in hippocampal CA1 neurons. *Neuroscience* 113(3):617–628
76. Yamazaki Y, Fujii S, Nakamura T, Miyakawa H, Kudo Y, Kato H, Ito K (2002) Changes in  $[Ca^{2+}]_i$  during adenosine triphosphate-induced synaptic plasticity in hippocampal CA1 neurons of the guinea pig. *Neurosci Lett* 324(1):65–68
77. Somjen GG (2001) Mechanisms of spreading depression and hypoxic spreading depression-like depolarization. *Physiol Rev* 81(3):1065–1096
78. Yoshioka K, Saitoh O, Nakata H (2001) Heteromeric association creates a P2Y-like adenosine receptor. *Proc Natl Acad Sci U S A* 98(13):7617–7622
79. Yoshioka K, Saitoh O, Nakata H (2002) Agonist-promoted heteromeric oligomerization between adenosine A(1) and P2Y(1) receptors in living cells. *FEBS Lett* 523(1–3):147–151
80. Yoshioka K, Hosoda R, Kuroda Y, Nakata H (2002) Hetero-oligomerization of adenosine A1 receptors with P2Y1 receptors in rat brains. *FEBS Lett* 531(2):299–303
81. Moore KA, Nicoll RA, Schmitz D (2003) Adenosine gates synaptic plasticity at hippocampal mossy fiber synapses. *Proc Natl Acad Sci U S A* 100(24):14397–14402
82. Frenguelli BG, Llaudet E, Dale N (2006) Real-time measurements of ATP and adenosine release during oxygen-glucose deprivation in area CA1 of rat hippocampal slices. Paper presented at the 8th International Symposium on Adenosine and Adenine Nucleotides, University of Ferrara, Ferrara, Italy, 24–28 May 2006
83. Troadec JD, Thirion S, Petturiti D, Bohn MT, Poujeol P (1999) ATP acting on P2Y receptors triggers calcium mobilization in primary cultures of rat neurohypophysial astrocytes (pituicytes). *Pflugers Arch* 437(5):745–753
84. Schipke CG, Boucein C, Ohlemeyer C, Kirchhoff F, Kettenmann H (2002) Astrocyte  $Ca^{2+}$  waves trigger responses in microglial cells in brain slices. *FASEB J* 16(2):255–257
85. Dirnagl U, Iadecola C, Moskowitz MA (1999) Pathobiology of ischaemic stroke: an integrated view. *Trends Neurosci* 22(9):391–397
86. Volonte C, Merlo D (1996) Selected P2 purinoceptor modulators prevent glutamate-evoked cytotoxicity in cultured cerebellar granule neurons. *J Neurosci Res* 45(2):183–193
87. Zona C, Marchetti C, Volonte C, Mercuri NB, Bernardi G (2000) Effect of P2 purinoceptor antagonists on kainate-induced currents in rat cultured neurons. *Brain Res* 882(1–2):26–35
88. Cavaliere F, D'Ambrosi N, Ciotti MT, Mancino G, Sancesario G, Bernardi G, Volonte C (2001) Glucose deprivation and chemical hypoxia: neuroprotection by P2 receptor antagonists. *Neurochem Int* 38(3):189–197
89. Cavaliere F, D'Ambrosi N, Sancesario G, Bernardi G, Volonte C (2001) Hypoglycaemia-induced cell death: features of neuroprotection by the P2 receptor antagonist basilin blue. *Neurochem Int* 38(3):199–207